Improved lipid profile through liver-specific knockdown of liver X receptor α in KKAy diabetic mice

Joerg F. Rippmann,[2],* Corinna Schoelch,[2],† Thomas Nolte,§ Heidi Pavliska,** André van Marle,** Helmuth van Es,[1],** and Juergen Prestle[3],†

From the Department of Pulmonary Diseases Research,* Department of Metabolic Diseases Research,† and Department of Nonclinical Drug Safety,§ Boehringer Ingelheim Pharma GmbH & Co. KG, 88397 Biberach, Germany; and Biofocus-DPI,** 2333 CN Leiden, The Netherlands

Abstract Nuclear hormone receptors liver X receptor (LXRα and LXRβ) ligands are attractive approaches for the treatment of dyslipidemia and atherosclerosis. To further elucidate the function of LXRα in liver lipid metabolism in a disease-relevant animal model, the KKAy mouse, we used adenoviral vectors to selectively knock down LXRα gene expression. Out of five different short hairpin RNAs (shRNAs) that were tested in vitro, one construct was selected for detailed analysis of LXRα knockdown in vivo. Reduction of LXRα transcript levels to 48 ± 13% compared with control virus transduction resulted in a significant downregulation of the LXRα-regulated lipogenic genes sterol-regulatory element binding protein-1c (SREBP1c) and stearoyl CoA desaturase 1 in vivo. Interestingly, ABCA1 and phoshoenol-pyruvate carboxykinase 1 expression was not affected, whereas lipoprotein lipase (LPL) expression was found to be increased. In addition, 8 days after virus transduction, both plasma and liver triglycerides (TGs) were reduced by about 50%. Changes in TG levels were not due to reduced food intake in virus-treated animals, because pair-fed mice showed unchanged TG levels. Taken together, liver-specific knockdown of LXRα in vivo by shRNA reduced expression of lipogenic master genes, like SREBP1c, and improved the lipid profile of hypertriglyceridemic KKAy mice.—Rippmann, J. F., C. Schoelch, T. Nolte, H. Pavliska, A. van Marle, H. van Es, and J. Prestle. **Improved lipid profile through liver-specific knockdown of liver X receptor α in KKAy diabetic mice.** *J. Lipid Res.* 2009. **50**: 22–31.

Supplementary key words nuclear hormone receptor • hypertriglyceridemia • short hairpin RNA • adenoviral gene transfer • triglycerides • gene expression

Disorders in lipid metabolism still represent a major unmet medical need. Lipid disorders are main risk factors for cardiovascular diseases like atherosclerosis, which is the leading cause of death in industrialized countries. Statins, drugs that inhibit HMG-CoA reductase, are effective in lowering LDL cholesterol levels, but they have only moderate effects on plasma triglyceride (TG) and HDL-cholesterol levels.

The nuclear hormone receptors liver X receptors LXRα and LXRβ are important cellular cholesterol sensors. Activated by oxygenated sterols, they form obligate heterodimers with retinoid X receptor and regulate expression of genes involved in cholesterol and lipid metabolism, as well as glucose homeostasis and inflammation (as reviewed in Refs. 1, 2). LXRα and LXRβ have both complementary and autonomous functions (3, 4). This is also reflected by differential tissue expression of both isoforms. In the adult mouse, LXRα is the predominant isoform in liver, adipose tissue, and macrophages, whereas LXRβ is expressed ubiquitously at lower levels (5).

Small-molecule LXR agonists have gained attention owing to their putative anti-atherosclerotic effects: LXR agonists promote reverse cholesterol transport in vivo, that is, the elimination of cholesterol from foam cells in the vascular wall and transport to the liver via HDL particles for secretion as bile acids (6). The downside of unspecific pharmacological LXR activation is an induction of lipogenesis in the liver, which causes hypertriglyceridemia and liver steatosis (7, 8). At the molecular level, the positive therapeutic effect is exemplified by gene induction of members of the ABC superfamily of membrane transporters driving the reverse cholesterol transport, for example, ABCA1. Upregulation of the transcription factor sterol-regulatory element binding

Abbreviations: ALP, alkaline phosphatase; AST, aspartate aminotransferase; ChREBP, carbohydrate response element binding protein; CYP7a, cholesterol 7α-hydroxylase; FASN, fatty acid synthase; LDH, lactate dehydrogenase; LPL, lipoprotein lipase; LXR, liver X receptor; PCK1, phosphoenolpyruvate carboxykinase 1; SCD1, stearoyl CoA desaturase 1; shRNA, short hairpin RNA; SREBP1c, sterol-regulatory element binding protein-1c; TC, total cholesterol; TG, triglyceride; 22-*S*-HC, 22-*S*-hydroxycholesterol.

[1] Present address of H. van Es: Stem Cell Innovations, 2333 BZ Leiden, The Netherlands.

[2] J. F. Rippmann and C. Schoelch contributed equally to this work.

[3] To whom correspondence should be addressed.
    e-mail: juergen.prestle@bc.boehringer-ingelheim.com

protein-1c (SREBP1c) and carbohydrate response element binding protein (ChREBP), on the other hand, drives the lipogenic gene program (7–10).

Transgenic mice with a targeted deletion of LXRα and LXRβ, as well as double knockouts, have been generated (11, 12). LXRβ-deficient mice, unlike LXRα-deficient mice, do not display a hepatic phenotype, confirming the prominent role of LXRα in liver. Transgenic mice with a liver-specific overexpression of LXRα have been described as well (13). Moreover, an interesting combinatorial approach using different synthetic LXR modulators in LXR subtype-specific knockout animals has recently been published (14). Double knockouts of LXRα and apoE have recently been shown to exhibit massive cholesterol accumulation in peripheral tissues and accelerated atherosclerosis. This phenotype could be overcome by pharmacological activation of LXRβ, demonstrating that LXRβ could compensate for the loss of LXRα in that respect (15). Altogether, genetic and pharmacological evidence not only supports the concept of subtype or tissue-specific LXRβ agonists for the treatment of atherosclerosis, but conceptually opens the possibility of developing LXRα-specific antagonists for the treatment of hypertriglyceridemia.

Transgenic animals, however, hamper the limitation of possible developmental adaptation. In the present study, we describe an interventional genetic approach in a disease-relevant animal model. For the first time, Ad5-mediated gene transfer was used to specifically knock down LXRα mRNA in vivo using short hairpin RNA (shRNA) (Ad5-shRNA-LXRα). KKAy mice were chosen as an established animal model characterized by hyperglycemia, hypercholesterolemia, and severe hypertriglyceridemia (16). We analyzed plasma lipid parameters and measured gene expression of established LXR target genes.

METHODS

Cell culture

For in vitro studies of the LXRα knockdown effects, the mouse hepatic cell line FL83B (American Type Culture Collection #CRL-2390) was chosen. The cells were cultured at 37°C with 5% CO_2 in Ham's F12K medium with 2 mM L-glutamine adjusted to contain 1.5 g/l sodium bicarbonate and 10% FBS and were split 1:5 twice a week. For transduction experiments, 4×10^5 cells per well were seeded in a 6-well plate at a 50% confluence 24 h prior to transduction with adenovirus. Infected cells were incubated for at least 2 days until harvest. For the combined treatment with adenovirus and LXRα agonist, cells were cultured for an additional 24 h in the presence of T0901317 (8).

Adenovirus production and purification

For the generation of recombinant Ad5 adenoviruses, pIPspAdapt-based constructs were transiently transfected in a 96-well format together with the adenoviral helper DNA into producer cells Per.C6/E2A (17). The resulting adenoviruses were propagated by reinfection of Per.C6/E2A. Crude virus was obtained from the growth medium 5–10 days post infection after repetitive freeze–thaw cycles and centrifugation (5 min, 1,500 g) to lyse the cells and to remove cell debris, respectively. Pure virus batches were obtained by harvesting infected cells prior to their lysis 5 days

post infection, using 0.5% sodium deoxycholate. After removal of cell debris by centrifugation, virus was isolated by sequential use of a CsCl step gradient (58,400 g for 2 h in a SW41 rotor; Beckman Instruments, Palo Alto, CA) and an isopycnic CsCl centrifugation (260,000 g for 16 h in an NVT 90 rotor, Beckman). The virus was then subjected to three consecutive dialysis steps in PBS (pH 7.4, GIBCO-Life/Invitrogen) supplemented to contain: 5% sucrose, 0.68 mM $CaCl_2$, and 0.65 mM $MgCl_2$. Titers of the crude lysates and pure virus preparations were determined by real-time PCR analysis as previously described (18). Infectious units were determined using the Adeno-X™ Rapid Titer Kit (BD Clontech). Typically, the ratio of virus particles to infectious units varied between 30 and 100.

Western blot analysis

For the analysis of protein expression, ∼50 mg tissue was homogenized in a FastPrep® FP120 tissue homogenizer (MP Biomedicals) in PBS, 10 mM mercaptoethanol, and proteinase inhibitor (complete, Roche Diagnostics). Protein concentration was determined by Bradford analysis (BioRad), and 20 µg protein lysate was separated on a 4–12% gradient SDS-PAGE (NuPage) and transferred to Protran-nitrocellulose membrane (Perkin-Elmer). Blots were blocked in 137 mM NaCl, 5% milk powder, and 20 mM Tris, pH 7.6 (5% milk in Tris-buffered saline), and incubated with anti-β-galactosidase (1:1,000; Rockland), washed three times with 1 × TBS/0.1% Tween20, and incubated with anti-rabbit HRP-conjugated secondary antibody (1:1,000; Amersham Biosciences). Immunoreactive bands were visualized using ECL (Amersham Biosciences).

Gene expression analysis

For quantitative gene expression analysis, total RNA was isolated from either cell culture lysates or tissue samples according to the RNeasy protocol (Qiagen). Briefly, cells were rinsed with PBS and lysed directly in the 6-well plate with 700 µl of RLT lysis buffer. Genomic DNA was sheared by centrifugation of the lysate through Qiashredder™ spin columns (10,000 g, 2 min, Qiagen), and the RNA was precipitated by the addition of 1 vol 70% ethanol. The precipitate was loaded on an RNeasy spin column (Qiagen), DNase treated, and eluted in 60 µl diethylpyro-carbonate-H_2O according to the manufacturer's protocol. The purified total RNA was stored at −20°C. For the RNA isolation from animal tissue, fresh samples (∼50 mg) were transferred into Fast Prep homogenization tubes (green cap, Qbiogen) together with 700 µl of RLT lysis buffer and homogenized at speed 6.5 for 20 s. Prior to RNA precipitation and isolation, the samples were phenol and chloroform extracted by consecutive addition of 1 vol of the organic solvents, mixing, and phase separation by centrifugation (room temperature, 10,000 g, 2 min). The gene expression levels were determined by TaqMan® analysis in a 7900HT Sequence Detection System (Applied Biosystems) using the TaqMan® EZ RT-PCR reagent kit (Applied Biosystems) for reverse transcription and PCR amplification in an ABI PRISM 384-well optical reaction plate (Applied Biosystems; see **Table 1** for primer sequence identities). Relative quantities of expression levels were determined by comparison of cycles of threshold values with a dilution series of a standard total RNA sample and normalized for the 18S rRNA quantity. For the presentation of the expression levels, normalized relative quantities of a transcript were divided by the mean value of the respective control group and displayed as percent control values.

Animal treatment

Male KKAy mice [KKAy/Ta Jcl] weighing 40 ± 5 g (approximately 10 weeks old) were purchased from Clea (Japan). These

TABLE 1. Short hairpin RNA sequences for the knockdown of murine transcripts

Insert Name	Target Sequence
LXRα_v1	CAGATCCGCTTGAAGAAAC
LXRα_v2	CACACATATGTGGAGGCCC
LXRα_v3	GTGTTTGCCCTTCGCCTGC
LXRα_v4	CAGCTCCCTGGCTTCCTAC
LXRα_v5	CTACATGCGGCGGAAATGC
Luc_v	GGTTACCTAAGGGTGTGGC

LXRα, liver X receptor α. The short hairpin RNA sequences were cloned as inverse complementary constructs with a let7 loop and the guiding strand following the complementary sequence. Expression is controlled by a human U6 promoter.

mice were originally generated by repeated cross-breeding of yellow obese mice with KK mice (19). Nakamura (20) disclosed the characteristics of diabetes mellitus in an inbred strain of mice named KK. The yellow obese mice bear a dominant gene of Ay, which shows yellow coat color in heterozygous form. The yellow Ay mutation produces a mouse that also presents hyperinsulinemia, insulin resistance, leptin resistance, hyperglycemia, and hyperleptinemia. The cross-breed of both strains, the KKAy mouse, is a model of obesity, hypertriglyceridemia, and hypercholesteremia and also shows severely elevated plasma glucose and insulin levels, and is therefore diabetic and insulin resistant (16).

The mice were conventionally housed in Makrolon type II cages at a constant temperature of $22 \pm 3°C$, on a 12 h light/dark cycle. Mice were fed a standard chow diet, and food and water were provided ad libitum. Ad5 vector samples were diluted in PBS injection buffer [150 mM NaCl, 1 mM $CaCl_2$, 0.5 mM $MgCl_2$, 0.5% (w/v) sucrose, and 50 mM H_2PO_4, pH 7.4] and injected intravenously via the tail vein. An additional group of animals had been pair-fed versus each of the different shRNA-treated and control groups. Prior to euthanization, animals were starved for 5 h to standardize nutrition status at the time of analysis. Blood samples were obtained by puncture of the retro-orbital vein plexus under isoflurane anesthesia to determine TGs, total cholesterol (TC), total bilirubin, lactate dehydrogenase (LDH), alkaline phosphatase (ALP), and aspartate aminotransferase (AST). Blood samples (10 μl) for the determination of blood glucose were taken from the tip of the tail. Animals were euthanized by dislocation of the neck, and tissue samples were collected thereafter. All experimental procedures were conducted according to the German Animal Protection Law and were approved by the Animal Review Committee of the German government.

Analytical procedures

Standard procedures were used to determine blood parameters using an automated analyzer according to the manufacturer's instructions (Cobas Integra 400; Roche Analytics, Germany).

Histology of liver tissues

For the analysis of LacZ expression and lipid load, liver samples were frozen in Tissue-Tek (Sakura) on dry ice and stored at −80°C until cryosections of 10 μm were prepared on a Leica CM 30506S cryotome. For the analysis of the β-galactosidase activity, samples were fixed in 2% paraformaldehyde for 30 min. Cells were permeabilized by incubation in 0.1% Triton X-100 for 10 min. After each step, samples were rinsed in PBS. The staining solution was always freshly prepared by addition of 0.2% of X-Gal in DMSO to the prepared staining buffer [2 mM $MgCl_2$, 5 mM $K_4Fe(CN)_6$, 5 mM $K_3Fe(CN)_6$ in PBS]. Samples were incubated in the staining solution for 5 h at room temperature, rinsed in PBS, and mounted in 90% glycerol. The enzymatic

activity of β-galactosidase was detected as a nuclear blue staining, owing to the nuclear localization signal at the N-terminus of the construct. For detection of tissue lipid load and histology, the cryosections were fixed for 1 h in 10% formalin and rinsed three times with ddH_2O. Samples were dehydrated for 5 min in 100% propylene glycol, stained with 0.5% Oil Red O in propylene glycol for 1 h at room temperature, and rinsed in 85% propylene glycol and ddH_2O for 5 min. For nuclear staining, samples were incubated for 5 min at room temperature in Mayers' hemalaun solution (Merck), rinsed in ddH_2O, and counterstained with 1% eosin solution for 3 min. After a final rinsing in ddH_2O, sections were mounted with Aquatex (Merck). Samples were analyzed on a Zeiss Axiovert 40CFL microscope, and images were recorded by AxioVision software, version 4.5.

Statistical analysis

Results are given as means $\pm$ SD. For group comparisons, the unpaired Student's t-test was used. When testing for changes in single parameters in individual groups over time, one-factor ANOVA for repeated measurements was used. Longitudinally observed parameters in different groups were compared by two-factor ANOVA for repeated measurements. The ANOVA was followed by posthoc analysis with Bonferroni's correction for multiple comparisons. Parameters with values $P < 0.05$ were considered to differ statistically significantly.

RESULTS

In vitro characterization of Ad5-LXRα-shRNA vectors by transduction of FL83B cells

For the interference with the LXRα gene expression, a set of five different LXRα-shRNAs, one green fluorescent protein reporter, and one shRNA control (designed to target the firefly luciferase transcript without significant sequence matches to the mouse genome) adenovirus vectors were constructed. These vectors (LXRα_v1, LXRα_v2, LXRα_v3, LXRα_v4, and LXRα_v5), and shRNA sequence reference (see **Table 2**) were first tested in an in vitro cell culture system for their efficiency to knock down LXRα mRNA, as well as for the downstream effects putatively related to reduced expression of this nuclear hormone receptor. To this end, the mouse cell line FL83B, which is of hepatic origin, is able to respond to the treatment of LXR-specific agonists, like T0901317. Relative mRNA expression of LXRα in this cell line is 1.8-fold higher than LXRβ expression, as assessed by real-time PCR analysis (data not shown). In a first series of experiments, the transduction procedure of this cell line was optimized using a crude adenovirus preparation carrying the GFP reporter construct. At a multiplicity of infection of 1,000, approximately 80% of the cells were found to be GFP positive (data not shown). In further in vitro experiments, this ratio of vector genomes to seeded cells was kept constant.

To identify the most efficient knockdown vectors, FL83B cells were transduced two times independently with crude lysate preparations of five different LXRα knockdown vectors. The knockdown efficiencies were analyzed on mRNA levels with specific quantitative RT-PCR probes and compared with Luc_v-treated cells, which served as controls. The vectors LXRα_v4 and LXRα_v3 were the two most

Gene	Forward Primer (5′–3′)	Reverse Primer (5′–3′)	Probe (5′FAM–TAMRA3′)
SCD1	CGTTCCAGAATGACGTGTACGA	GCGTGTGTTTCTGAGAACTTGTG	CCGAGATCACCGCGCCCA
FASN	CATTGGTGGTGTGGACATGGT	GACCGCTTGGGTAATCCATAGA	CCCAGCCTTCCATCTCCTGTCATCATCT
PCK1	CCGCTGGATGTCGGAAGA	TGCTGAATGGGATGACATACATG	AAGCATTCAACGCCAGGTTCCC
SREBP1c	CIACGGAGCCATGGATTG	AAGTCACTGTCTTGGTTGTTGATGAG	ACATTTGAAGACATGCTICA
LXRα	CAACGGAGTTGTGGAAGACAGAACCTCAA	TCCCTGAGGATGCAAGTGTTG	TGCCTGATGTTTCTCCTGATTCT
CYP7a	GGAATAAGGAGAAGGAAAGTAGGTGAA	TTCAAGAGGATTGGATCCGAACT	ACGGGTTGATTCCATACCTGGGCTGT
LPL	GGGAAATGATGTGGCCAGATT	GTACCCTAAGAGGTGGACGTTGTCT	ACTGGATGGAGGAGGAGTTTAACTACCCC

SCD1, stearoyl CoA desaturase 1; FASN, fatty acid synthase; LPL, lipoprotein lipase; PCK1, phosphoenolpyruvate carboxykinase 1; SREBP1c, sterol-regulatory element binding protein-1c; CYP7a, cholesterol 7α-hydroxylase. Gene-specific probes were labeled with 6-FAM™ and TAMRA for internal quenching. Mn^{+2} concentrations were optimized to reach 100% amplification efficiency according to the manufacturer's instructions. The following sequence detection kits were designed by Applied Biosystems: Eucaryotic 18S rRNA (#Hs99999901_s1), ABCA1_murine (#Mm00442646_m1), LXRβ_murine (#Mm00437262_m1), ChREBP_murine (#Mm02342723_m1), Angptl3_murine (#Mm00803820_m1), CD68_murine (#Mm03047342_m1), and CD115_murine (#Mm01266652_m1).

efficacious constructs, with remaining LXRα mRNA levels of 30 ± 4% and 36 ± 1%, followed by vectors LXRα_v2 (53 ± 6%), LXRα_v5 (57 ± 12%), and LXRα_v1 (70 ± 6%). The purified adenovirus vectors LXRα_v3 and LXRα_v4 were even more effective and reduced LXRα gene expression to 13 ± 4% (LXRα_v3) or 28 ± 8% (LXRα_v4), compared with control-treated FL83B cells (**Fig. 1A**). This also affected the expression of corresponding responsive genes, like SREBP1c and stearoyl CoA desaturase 1 (SCD1), which showed an approximately 50% reduced expression level compared with control-treated cells. The expression of fatty acid synthase (FASN) was only marginally reduced, suggest-

ing that this gene is under transcriptional control of LXRβ, rather than LXRα (Fig. 1A).

Treatment of FL83B cells with the nonspecific LXR agonist T0901317 did not influence LXRα expression but stimulated expression of SREBP1c, SCD1, and FASN by 509%, 245%, and 186%, respectively, in the Luc_v-treated control group (data not shown).

LXRα_v3 and LXRα_v4 knockdown vectors were also effective in the presence of the LXR agonist. The expression profile of the respective target genes SREBP1c, SCD1, and FASN was more or less the same as without the treatment of T0901317. Gene expression levels were compared
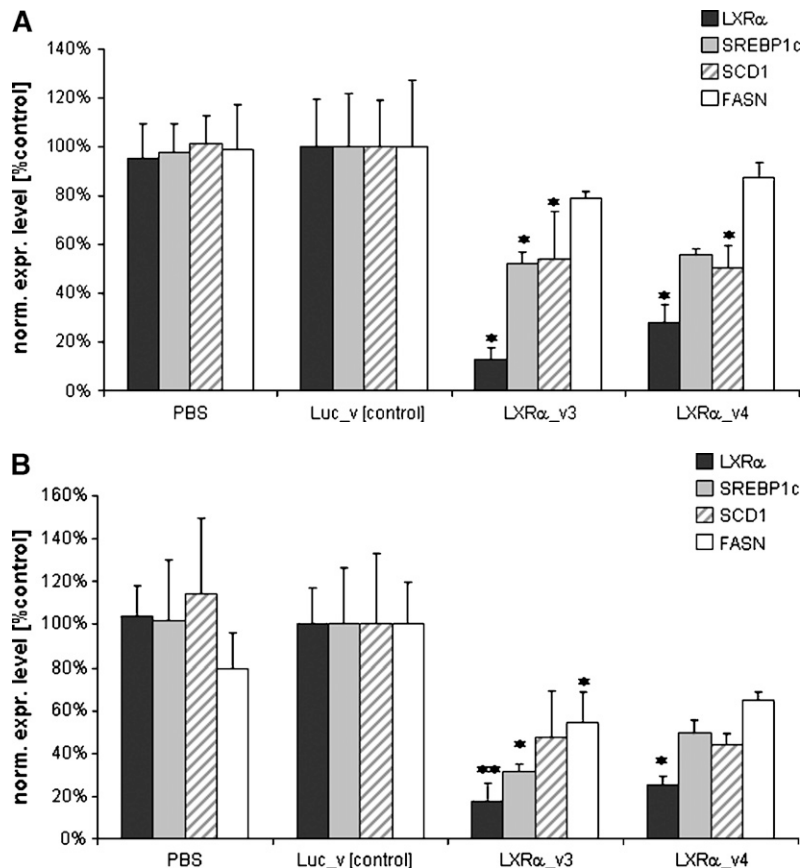

Fig. 1. Ad5-mediated knockdown analysis of liver X receptor α (LXRα) and responsive genes in FL83B cell cultures. FL83B cells were seeded to 50% confluence and transduced with Ad5 constructs at a multiplicity of infection of 1,000. The cells were harvested, and the expression levels of LXRα, sterol-regulatory element binding protein-1c (SREBP1c), stearoyl CoA desaturase 1 (SCD1), and fatty acid synthase (FASN) were determined by qRT-PCR. Expression values are calculated as percent of luciferase control adenovirus vector (Luc_v)-treated FL83B cells in each experiment. A: Basal gene expression levels in FL83B cell cultures 48 h after transduction in the presence of LXRα gene knockdown or control vectors. B: Gene expression levels in the presence of LXRα gene knockdown 72 h after virus transduction in combination with the LXR agonist treatment (T0901317, 1 μM, 24 h). Treatment with T0901317 per se did not influence LXRα expression but stimulated expression of SREBP1c, SCD1, and FASN by 509%, 245%, and 186%, respectively, in Luc_v-treated control group (not depicted). Bars represent means ± SD of three independent experiments. Significant differences to Luc_v control group according to Student's t-test: * $P < 0.05$, ** $P < 0.01$.

between LXRα knockdown vector- and Luc_v control vector-treated cultures. In the LXRα_v3 group, expression of LXRα, SREBP1c, SCD1, and FASN was reduced to 18%, 31%, 47%, and 55%, respectively. In the LXRα_v4-treated cultures, LXRα, SREBP1c, SCD1, and FASN expression was knocked down to 25%, 49%, 44%, and 64%, respectively. In conclusion, treatment of FL83B cells with LXRα knockdown vectors antagonized the effect of the potent LXR agonist T0901317.

Identification of efficient Ad5 vector dose for in vivo treatment of KKAy mice

For the in vivo knockdown studies, the appropriate adenovirus dose was identified by tail vein injection of different amounts of adenovirus vectors encoding the reporter gene LacZ. Three days post injection, liver sections of transduced KKAy mice were analyzed for the presence of β-galactosidase expression (**Fig. 2**). At an Ad5 titer of 1×10^{11} vector genomes per animal (Fig. 2B), a clear nuclear staining of over 70% of the hepatocytes could be detected. Increasing titers above this level led to organ toxicity, as determined by considerably elevated LDH levels in the serum of those animals (data not shown). A virus titer of 1×10^{11} viral genomes/animal was therefore chosen for further experiments. The tissue tropism of the adenovirus vectors was analyzed by Western immunoblot of different organ homogenates (Fig. 2C). In all animals treated with 1×10^{11} viral genomes/animal, a strong signal in liver samples could be detected. The visceral adi-

pose tissue homogenates of some animals gave a very faint signal of the β-galactosidase protein.

In vivo knockdown LXRα in KKAy mice with Ad5-shRNA-LXRα

At the age of 10 weeks, male KKAy mice were injected via the tail vein with 1×10^{11} vector genomes per animal. To distinguish virus treatment-related effects from LXRα-specific knockdown effects, a buffer control group, together with a group of animals that received an Ad5 vector expressing an shRNA against the firefly luciferase transcript, was used, and animals were analyzed at day 8 post injection.

First, in vivo experiments were carried out with LXRα_v3, LXRα_v4, and Luc_v control vector. Similar to LacZ_v, treatment of the KKAy mice with a dose of 1×10^{11} Luc_v control vector genomes per animal did not lead to an acute liver toxicity as analyzed by LDH, ALP, and AST activity in the plasma (**Table 3**). Treatment of the KKAy mice with 1×10^{11} adenovirus vector LXRα_v4 led to a moderate increase in AST and LDH plasma activity. With vector LXRα_v3, liver enzymes were dramatically enhanced (Table 3). Cryosections of liver tissue were prepared from all experimental groups and stained for lipid load and gross morphology. Sections of PBS-treated animals showed punctuated lipid staining mainly around central veins (**Fig. 3**). Treatment with adenovirus Luc_v and LXRα_v4 led to a slight degeneration of centrolobular hepatocytes and morphological findings probably resem-
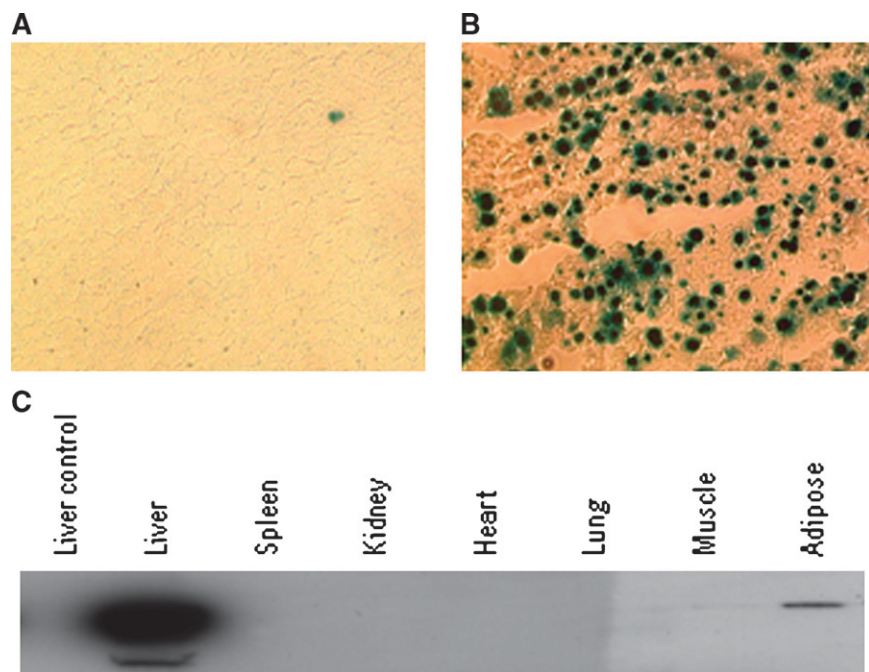

Fig. 2. Liver transduction of KKAy mice with adenoviral expression vector for β-galactosidase. Male KKAy mice were injected intravenously with different doses of Ad5 particles harboring an expression cassette for the NLS-LacZ gene. Animals were injected with 1×10^{10} (A) or 1×10^{11} (B) virus genomes per animal. Three days post transduction, animals were euthanized and liver sections were stained for β-galactosidase activity. C: Western immunoblot analysis of tissue homogenates from an animal that received 1×10^{11} virus genomes via the tail vein showing β-galactosidase protein.

TABLE 3. Plasma analysis of PBS-, Luc_v-, LXRa_v4-, and LXRa_v3-treated and pair-fed animals 8 days post transduction

Test	PBS	Luc_v	LXRα_v4	LRXα_v3
LDH [U/L]	259 ± 51	388 ± 67	2,852 ± 685***	7,524 ± 2,265***
ALP [U/L]	156 ± 23	141 ± 27	332 ± 78	6,515 ± 2,964***
AST [U/L]	82 ± 18	90 ± 17	627 ± 203***	2,028 ± 737***
Pair-feeding	vs. PBS	vs. Luc_v	vs. LXRα_v4	vs. LXRα_v3
LDH [U/L]	167 ± 37	267 ± 223	290 ± 117	177 ± 34
AST [U/L]	52 ± 12	75 ± 36	73 ± 36	73 ± 18

LDH, lactate dehydrogenase; U/L, units per liter; ALP, alkaline phosphatase; AST, aspartate aminotransferase. Male KKAy mice (40 ± 5 g) were injected intravenously either with 1×10^{11} vector genomes per animal (n = 5) or with PBS injection buffer (n = 5). Additional groups were pair-fed to each shRNA-treated and control mice. Animals were euthanized 8 days post transduction and plazma enzymatic activity of LDH, ALP, and AST was determined. Data are represented as means ± SD. Significant differences from Luc_v group provided by ANOVA: *** $P < 0.001$.

bling Kupffer cell activation and oval cell proliferation. These changes were much more pronounced in LXRα_v3-treated animals, with putatively marked Kupffer cell activation and oval cell proliferation. The original structure of the liver cell plates was disarrayed to a large extent, and the staining of the lipid droplets was disperse (Fig. 3).

Because of the evident liver toxicity of the LXRα_v3 vector, only LXRα_v4 vector was used to further analyze gene expression profile and plasma parameters after LXRα knockdown. The PBS and Luc_v groups showed comparable expression levels of all genes (**Fig. 4**), and the Luc_v group was used for the normalization of the gene expression data. The animals that received the LXRα_v4 vector showed a reduction of the LXRα transcript level to 48 ± 13% compared with the Luc_v-treated control group (Fig. 4A). Expression of LXRβ was slightly higher in the PBS control group, which suggests that virus infection per se might reduce LXRβ expression (Fig. 4B). The reason for this remains unclear. It was evident, however, that LXRβ gene expression levels were much more variable within experimental groups, as compared

with LXRα gene expression. The LXR-responsive genes SREBP1c, SCD1, and Angpt13 followed in their respective transcription levels the gradual expression of LXRα, with SCD1 showing the most pronounced downregulation (Fig. 4A). Interestingly, LXR-responsive genes cholesterol 7α-hydroxylase (CYP7a), ChREBP, phosphoenolpyruvate carboxykinase 1 (PCK1), and ABCA1 were not significantly altered by specific LXRα knockdown (Fig. 4B). Most dramatic changes in gene expression were detected with LPL, another LXR target gene, which was increased almost 3-fold (21). Because LPL is barely expressed in normal liver, the increase in LPL expression in LXRα_v4 vector-treated animals might also be attributed to the already described activation of Kupffer cells/macrophages, which highly express LPL. To confirm this hypothesis, we analyzed gene expression of two additional macrophage marker genes, CD115 and CD68 (Fig. 4C). Both genes were found to be increased by about 2-fold and 3-fold in the LXRα_v4 vector treated group compared with Luc_v control group. This strongly suggests that increased LPL expression is a consequence of a higher number of macrophage cell types in
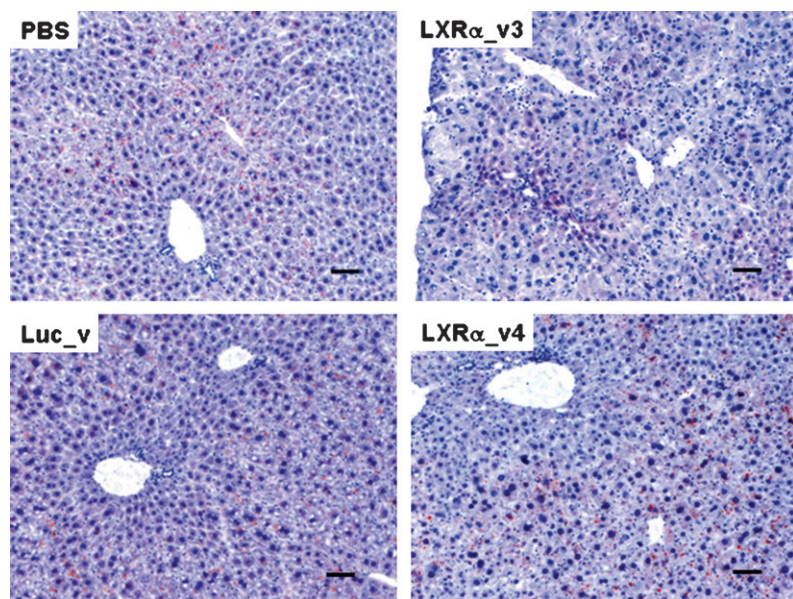
Fig. 3. Liver histology of animals treated with LXRα knockdown and control virus. Male KKAy mice (40 ± 5 g) were injected intravenously either with 1×10^{11} vector genomes per animal (n = 10) or with PBS injection buffer (n = 4). Animals were euthanized 8 days post transduction, and cryosections from liver samples were stained with Oil Red O and hematoxylin. Top left (PBS-treated control): normal liver tissue with Oil Red O-positive vacuoles predominantly in centrolobular region. Bottom left (treatment with Ad5 Luc_v) and bottom right (LXRα_v4-treated mouse): slight activation and proliferation of putative Kupffer cells; Oil Red O-positive vacuoles diffusely dispersed throughout the liver parenchyma. Top right (LXRα_v3-treated mouse): strong disorganization of liver cell plates as well as marked proliferation of putative Kupffer cells and oval cells; fine Oil Red O-positive vacuoles scattered throughout the liver parenchyma. Representative samples of treated animal groups (n = 5) are shown. Bars represent 60 μm.
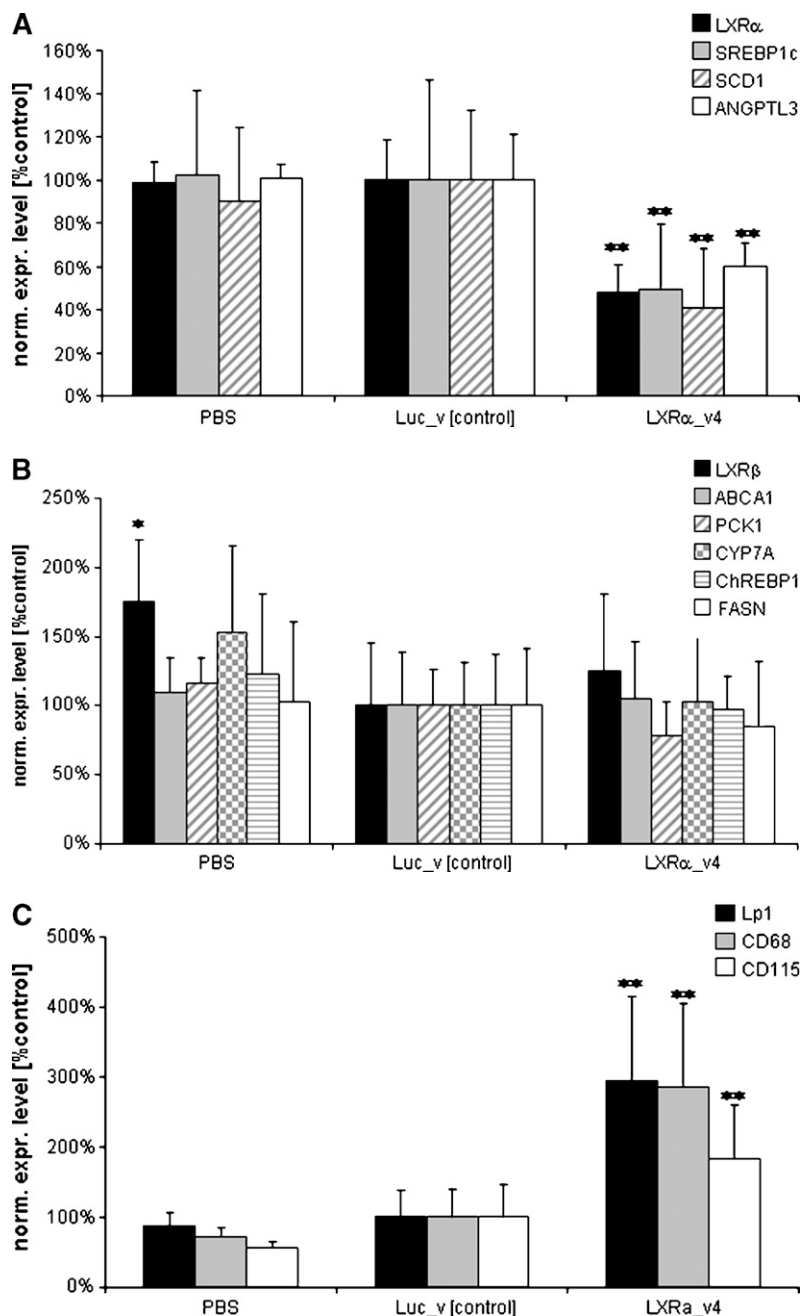
Fig. 4. Ad5-mediated knockdown analysis of LXRα and responsive genes in liver samples of KKAy mice. Male KKAy mice (40 ± 5 g) were injected intravenously either with 1×10^{11} vector genomes per animal (n = 10) or with PBS injection buffer (n = 4). Animals were euthanized 8 days post transduction, and gene expression levels in liver samples were analyzed by qRT-PCR. Expression levels of genes downregulated (A), not regulated (B), and upregulated (C) by LXRα knockdown virus are depicted as percent of Luv_v controls. Bars represent means + SD. Significant differences from Luc_v control group according to Student's t-test: * $P < 0.05$, ** $P < 0.01$.

the liver of LXRα knockdown animals (see also Fig. 3) and not of altered hepatic transcriptional control.

Physiological response of KKAy mice to treatment with LXRα knockdown vectors

Food consumption and body weight of KKAy mice were recorded continuously after virus administration. AdV transduction had a pronounced effect on food intake at day 1 after injection. Luc_v- and LXRα_v4-treated animals showed a reduction in food intake by 30–50% compared with the PBS-treated control group (**Fig. 5**). However, during the next days, the animals recovered and consumed similar amounts of food as PBS-treated animals. At the end of the experiment at day 8 post transduction, the

virus-treated animals consumed approximately 20% less food than the PBS control group.

Plasma TG, TC, and glucose levels were comparable between PBS- and Luc_v-treated animals at day 8 post transduction (**Fig. 6**). In the LXRα_v4 knockdown animals, plasma TGs were significantly reduced, by 52% (Fig. 6A). These changes in blood plasma lipids were reflected in a decrease in liver TG content to the same extent (Fig. 6B). Plasma glucose was reduced by 36% (Fig. 6C), whereas plasma TC levels (Fig. 6D) were similar between groups.

Because these metabolic parameters can readily be influenced by the feeding status of the animals, we also performed a pair-fed control experiment (Fig. 6). For a period of 8 days, separate groups of animals received each
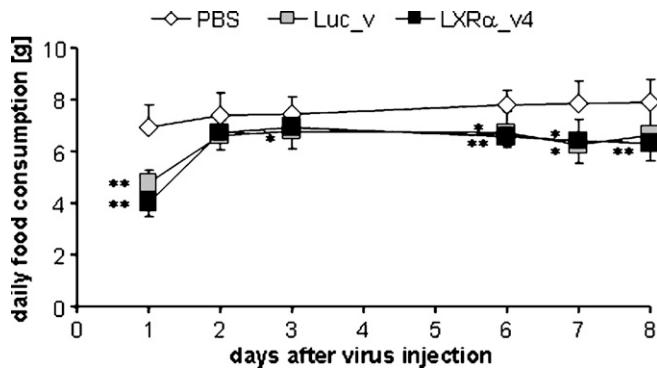
Fig. 5. Daily food consumption of KKA*y* mice treated with LXRα knockdown and control virus. Male KKA*y* mice (40 ± 5 g) were injected intravenously either with 1×10^{11} vector genomes per animal (n = 5) or with PBS injection buffer (n = 5). Animals were fed ad libitum with standard chow, and weight of food and animals was recorded once daily. Significant differences from PBS control group provided by ANOVA: * $P < 0.05$, ** $P < 0.01$. Data represent means ± SD.

DISCUSSION

From a pharmacological point of view, unspecific full LXR agonists, like T0901317, have been unsuccessful in the treatment of metabolic diseases because of lipid accumulation in the liver (7). Differential tissue distribution and individual cellular functions of LXRα and LXRβ provide the rationale for development of subtype-selective LXR modulators. Although LXRβ is an accepted molecular target for the treatment of atherosclerosis, the concept of LXRα antagonists for the treatment of dyslipidemia lacks in vivo proof of concept, so far. The primary goal of this study was thus to test the hypothesis that inhibition of LXRα in liver could possibly improve hypertriglyceridemic phenotype in a disease-relevant animal model. This study is the first to use LXRα subtype-selective shRNA-mediated knockdown in vivo to mimic pharmacological inhibition of LXRα specifically in liver with the result of lowering triglyceride levels in hypertriglyceridemic KKA*y* mice.

Effective shRNA constructs were first identified in vitro using hepatic cell line FL83B. The most efficacious virus, LXRα_v3, induced severe liver toxicity in vivo and was therefore not used for further analysis. A slight increase in liver enzymes LDH and AST was also seen with LXRα_v4 vector. However, histological analysis revealed no morphological difference between LXRα_v4 and Luc_v vector. We therefore consider the differences in gene expression
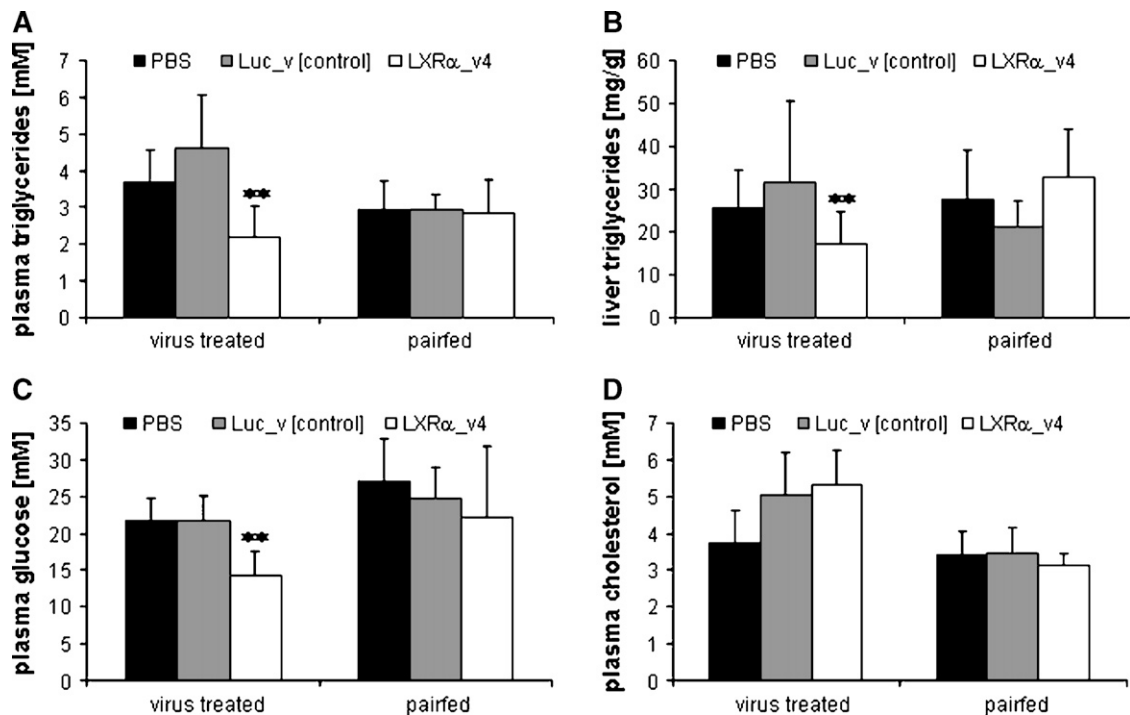
day exactly the same amount of food as the respective treatment groups had consumed the day before (see Fig. 5). In the pair-fed animals, no statistically significant differences in plasma and liver TG, TC, and plasma glucose could be detected between groups (Fig. 6).

Fig. 6. Plasma and liver triglycerides (TGs), plasma glucose, and plasma cholesterol levels of animals treated with LXRα knockdown and control virus and pair-fed animals. Male KKA*y* mice (40 ± 5 g) were injected intravenously either with 1×10^{11} vector genomes per animal (n = 5 per group) or with PBS injection buffer (n = 5 per group). Animals were fed ad libitum with standard chow during the experiment but starved for 5 h prior to euthanization. Control groups were pair-fed to each short hairpin RNA-treated and control-treated group with standard chow during the experiment but starved for 5 h prior to euthanization. Data are represented as means ± SD at 8 days post transduction. A: Plasma TG levels. B: Liver TGs. C: Plasma glucose levels. D: Total plasma cholesterol levels. No statistically significant difference in any parameter between any groups could be detected in the pair-feeding experiment. In the virus treatment group, statistically significant differences to Luc_v control group are provided by ANOVA: ** $P < 0.01$.

pattern and plasma parameters between these two constructs to be specific to the knockdown of LXRα. Whether the liver toxicity observed with LXRα_v3 in vivo is due to more-efficient knockdown of LXRα as compared with LXRα_v4 or to unspecific effects could not be analyzed. Although all shRNA constructs used in this study showed a discrimination of other transcripts with at least two mismatches in a Swiss-Waterman search against the ENSEMBL transcriptome, we cannot definitely exclude possible off-target effects described by others (22).

The pattern of changes in gene expression of LXR-responsive genes was comparable in vitro and in vivo. The lack of alterations in LXR-responsive genes PCK1, CYP7A, and ChREBP1 upon LXRα knockdown implies that these genes may be under specific control by LXRβ rather than LXRα. Of note, the ABCA1 gene was also not changed in LXRα shRNA-treated animals. This result strengthens the hypothesis that LXRβ is the more relevant subtype controlling ABCA1 transcription (23, 24). The present study therefore adds further support to the working hypothesis that it is possible to separate the favorable LXR-mediated anti-atherosclerotic properties from the unfavorable lipogenic effects.

Yet, mRNA expression of LXRα in liver of KKAy mice is 36-fold higher compared with LXRβ (data not shown), as assessed by TaqMan analysis, and there was no compensatory upregulation of LXRβ after knockdown of LXRα. It may therefore be simplistic to ascribe the role in regulation of LXR target genes to the LXRβ subtype, if expression of the gene of interest is not affected by the specific knockdown of the LXRα subtype, as described herein for PCK1, ABCA1, and other genes. Nuclear hormone receptors, like LXR, function in a ligand-dependent manner to recruit coregulator proteins to target gene promoters. In the absence of a ligand, corepressor proteins can be associated with LXR-repressing transcription of specific genes. Deleting the receptor, therefore, does not necessarily reflect the effect of an antagonist; or vice versa, the effect of an agonist does not necessarily reflect the upregulation of the receptor. It is the concerted action of nuclear hormone receptor, ligand, and a conglomeration of accessory coactivator/corepressor proteins that ultimately controls transcription of specific genes.

We found a significant increase in LPL expression and macrophage marker genes CD68 and CD115 in liver of LXRα_v4 vector-treated animals. As discussed before, and as shown in Fig. 3, adenoviral transduction per se stimulates host defense mechanisms, like Kupffer cell activation. However, the putative rise in macrophage number is specific to knockdown of LXRα, because expression of CD68 and CD155 is not statistically different between Luc_v control and the PBS group. Recent studies have demonstrated that LXR has anti-inflammatory activity (as reviewed in Ref. (1) and references therein). It can thus be speculated that knockdown of LXRα generates pro-inflammatory milieu in liver tissue, further facilitating macrophage infiltration.

Plasma TG levels strongly vary with the dietary status of the animal. Because food consumption was slightly reduced in the LXRα_v4 group on the last day of the study, we performed an additional experiment with a pair-feeding regimen. The blood analysis of the pair-fed animals revealed no difference in plasma TC, plasma TG, and liver tissue TG between groups. This confirms that the observed dramatic changes in the plasma lipid profile and liver TG content in the shRNA-treated animals are due to a specific downregulation of LXRα and accompanying responsive genes in the liver. In line with the present results, Kase et al. (25) recently demonstrated reduced lipogenesis in isolated human myotubes treated with an LXR antagonist. In their study, they used 22-S-hydroxycholesterol (22-S-HC), the synthetic stereoisomer to the endogenous LXR ligand 22-R-hydroxycholesterol, as an LXR antagonist. Myotubes were established from satellite cells isolated from muscle biopsies from lean, obese, and diabetic individuals. Lipid synthesis from acetate was reduced about 2-fold with 22-S-HC compared with baseline. Accordingly, expression of the lipogenic genes FASN and SCD1 was reduced 7-fold.

KKAy mice are characterized by a progressive increase in blood glucose and insulin levels from 5 weeks of age. Insulin sensitivity of adipose tissue decreases with age in these mice (26). We used 10-week-old KKAy mice with elevated plasma glucose levels reflecting their diabetic state. The plasma glucose levels were reduced in the LXRα_v4 group. Because PCK1 expression was not changed, other genes involved in glucose homeostasis may be altered in these animals (25). Again, a reduction in plasma glucose levels by LXRα knockdown is in line with the study by Kase et al. (25), who showed an increase in myocellular glucose uptake and oxidation with 22-S-HC.

A synthetic LXRα antagonist has not yet been described in vivo. Two independently developed LXRα knockout mice have been reported (11, 12). Both groups have analyzed the animals on normal chow diet as well as on chow diet supplemented with 0.2% to 2% cholesterol. Compared with results obtained in cholesterol-fed LXRα$^{-/-}$ mice, we find our data remarkably similar. Lipogenic genes SREBP1c and SCD1 are downregulated in all models. Although LXRα$^{-/-}$ mice on a normal diet show no obvious phenotype, feeding a diet with even mildly increased cholesterol content (0.2%) led to an accumulation of cholesterol in the livers. This was accompanied by increased liver mass and histological changes in the liver morphology characterized by macrophage infiltration and progressive hepatocellular degeneration. Peet et al. (11) also reported a dramatic increase in the serum levels of AST and ALP. However, the severe hepatic phenotype of LXRα$^{-/-}$ mice can be explained by the inability of these animals to cope with the additional dietary cholesterol. LXRα$^{-/-}$ mice are unable to upregulate CYP7a enzyme, which is crucial for metabolic clearance of excess dietary cholesterol as bile acids (27). The principal difference from our study is that we started the genetic intervention in animals with pre-existing fatty liver. We also detected no change in CYP7a gene expression level in the LXRα_v4 group; neither did we observe a further accumulation of cholesterol in liver in this group. If the liver toxic effects observed in our study

with LXRα_v3 are specific to downregulation of LXRα, the underlying pathophysiological mechanisms may thus be different between both models.

Together with genetic studies using knockout animals and pharmacological studies using synthetic LXR agonists, the present study expands our picture of LXRα function in liver metabolism. We show that LXRα is a key regulator of TG homeostasis and therefore principally supports the concept of specific LXRα antagonism in the treatment of hypertriglyceridemia. However, the downside of LXRα inhibition in liver may be the generation of a pro-inflammatory stimulus.▮

REFERENCES

1. Zelcer, N., and P. Tontonoz. 2006. Liver X receptors as integrators of metabolic and inflammatory signaling. *J. Clin. Invest.* **116:** 607–614.
2. Geyeregger, R., M. Zeyda, and T. M. Stulnig. 2006. Liver X receptors in cardiovascular and metabolic disease. *Cell. Mol. Life Sci.* **63:** 524–539.
3. Joseph, S. B., M. N. Bradley, A. Castrillo, K. W. Bruhn, P. A. Mak, L. Pei, J. Hogenesch, R. M. O'Connell, G. Cheng, E. Saez, et al. 2004. LXR-dependent gene expression is important for macrophage survival and the innate immune response. *Cell.* **119:** 299–309.
4. Steffensen, K. R., M. Nilsson, G. U. Schuster, T. M. Stulnig, K. Dahlman-Wright, and J. A. Gustafsson. 2003. Gene expression profiling in adipose tissue indicates different transcriptional mechanisms of liver X receptors alpha and beta, respectively. *Biochem. Biophys. Res. Commun.* **310:** 589–593.
5. Annicotte, J-S., K. Schoonjans, and J. Auwerx. 2004. Expression of the liver X receptor alpha and beta in embryonic and adult mice. *Anat. Rec. A Discov. Mol. Cell. Evol. Biol.* **277:** 312–316.
6. Naik, S. U., X. Wang, J. S. Da Silva, M. Jaye, C. H. Macphee, M. P. Reilly, J. T. Billheimer, G. H. Rothblat, and D. J. Rader. 2006. Pharmacological activation of liver X receptors promotes reverse cholesterol transport in vivo. *Circulation.* **113:** 90–97.
7. Grefhorst, A., B. M. Elzinga, P. J. Voshol, T. Plosch, T. Kok, V. W. Bloks, F. H. van der Sluijs, L. M. Havekes, J. A. Romijn, H. J. Verkade, et al. 2002. Stimulation of lipogenesis by pharmacological activation of the liver X receptor leads to production of large, triglyceride-rich very low density lipoprotein particles. *J. Biol. Chem.* **277:** 34182–34190.
8. Schultz, J. R., H. Tu, A. Luk, J. J. Repa, J. C. Medina, L. Li, S. Schwendner, S. Wang, M. Thoolen, D. J. Mangelsdorf, et al. 2000. Role of LXRs in the control of lipogenesis. *Genes Dev.* **14:** 2831–2838.
9. Cha, J. Y., and J. J. Repa. 2007. The liver X receptor (LXR) and hepatic lipogenesis. The carbohydrate-response element-binding protein is a target gene of LXR. *J. Biol. Chem.* **282:** 743–751.
10. Inaba, T., M. Matsuda, M. Shimamura, N. Takei, N. Terasaka, Y. Ando, H. Yasumo, R. Koishi, M. Makishima, and I. Shimomura. 2003. Angiopoietin-like protein mediates hypertriglyceridemia induced by liver X receptor. *J. Biol. Chem.* **278:** 21344–21351.
11. Peet, D. J., S. D. Turley, W. Ma, B. A. Janowski, J. M. Lobaccaro, R. E. Hammer, and D. J. Mangelsdorf. 1998. The LXRs: a new class of oxysterol receptors. *Cell.* **93:** 693–704.
12. Alberti, S., G. Schuster, P. Parini, D. Feltkamp, U. Diczfalusy, M. Rudling, B. Angelin, I. Bjorkhem, S. Pettersson, and J. A. Gustafsson. 2001. Hepatic cholesterol metabolism and resistance to dietary cholesterol in LXRbeta-deficient mice. *J. Clin. Invest.* **107:** 565–573.
13. Lehrke, M., C. Lebherz, S. C. Millington, H. P. Guan, J. Millar, D. J. Rader, J. M. Wilson, and M. A. Lazar. 2005. Diet-dependent cardiovascular lipid metabolism controlled by hepatic LXRalpha. *Cell Metab.* **1:** 297–308.
14. Lund, E. G., L. B. Peterson, A. D. Adams, M-H. N. Lam, C. A. Burton, J. Chin, Q. Guo, S. Huang, M. Latham, J. C. Lopez, et al. 2006. Different roles of liver X receptor alpha and beta in lipid metabolism: effects of an alpha-selective and a dual agonist in mice deficient in each subtype. *Biochem. Pharmacol.* **71:** 453–463.
15. Bradley, M. N., C. Hong, M. Chen, S. B. Joseph, D. C. Wilpitz, X. Wang, A. J. Lusis, A. Collins, W. A. Hseuh, J. L. Collins, et al. 2007. Ligand activation of LXRβ reverses atherosclerosis and cellular cholesterol overload in mice lacking LXRα and apoE. *J. Clin. Invest.* **117:** 2337–2346.
16. Castle, C. K., J. R. Colca, and G. W. Melchior. 1993. Lipoprotein profile characterization of the KKA(y) mouse, a rodent model of type II diabetes, before and after treatment with the insulin-sensitizing agent pioglitazone. *Arterioscler. Thromb.* **13:** 302–309.
17. Michiels, F., H. Van Es, L. Van Rompaey, P. Merchiers, B. Francken, K. Pittois, J. V. Der Schueren, R. Brys, J. Vandersmissen, F. Beirinckx, et al. 2002. Arrayed adenoviral expression libraries for functional screening. *Nat. Biotechnol.* **20:** 1154–1157.
18. Ma, L., H. A. Bluyssen, M. De Raeymaeker, V. Laurysens, N. Van der Beek, H. Pavliska, A-J. Van Zonneveld, P. Tomme, and H. H. Van Es. 2001. Rapid determination of adenoviral vectors titers by quantitative real-time PCR. *J. Virol. Methods.* **93:** 181–188.
19. Nishimura, M. 1969. Breeding of mice strains for diabetes mellitus. *Exp. Anim.* **18:** 147–157.
20. Nakamura, M., Yamamda, K. 1967. Studies on a diabetic (KK) strain of the mouse. *Diabetologia.* **3:** 212–221.
21. Zhang, Y., J. J. Repa, K. Gauthier, and D. J. Mangelsdorf. 2001. Regulation of lipoprotein lipase by oxysterol receptors, LXRα and LXRβ. *J. Biol. Chem.* **276:** 43018–43024.
22. Birmingham, A., E. M. Anderson, A. Reynolds, D. Ilsley-Tyree, D. Leake, Y. Fedorov, S. Baskerville, E. Maksimova, K. Robinson, J. Karpilow, et al. 2006. 3′UTR seed matches, but not overall identity, are associated with RNAi off-targets. *Nat. Methods.* **3:** 199–204.
23. Repa, J. J., S. D. Turley, J. A. Lobaccaro, J. Medina, L. Li, K. Lustig, B. Shan, R. A. Heyman, J. M. Dietschy, and D. J. Mangelsdorf. 2000. Regulation of absorption and ABC1-mediated efflux of cholesterol by RXR heterodimers. *Science.* **289:** 1524–1529.
24. Lund, E. G., J. G. Menke, and C. P. Sparrow. 2003. Liver X receptor agonists as potential therapeutic agents for dyslipidemia and atherosclerosis. *Arterioscler. Thromb. Vasc. Biol.* **23:** 1169–1177.
25. Kase, E. T., G. H. Thoresen, S. Westerlund, K. Højlund, A. C. Rustan, and M. Gaster. 2007. Liver X receptor antagonist reduces lipid formation and increases glucose metabolism in myotubes from lean, obese and type 2 diabetic individuals. *Diabetologia.* **50:** 2171–2180.
26. Iwatsuka, H., A. Shino, and Z. Suzuki. 1970. General survey of diabetic features of yellow KK mice. *Endocrinol. Jpn.* **17:** 23–30.
27. Janowski, B. A., P. J. Willy, T. R. Devi, J. R. Falck, and D. J. Mangelsdorf. 1996. An oxysterol signalling pathway mediated by the nuclear recpetor LXR alpha. *Nature.* **383:** 728–731.